GEOLOGICAL SURVEY OF CANADA
OPEN FILE 7852

Targeted Geoscience Initiative 4: Contributions to the Understanding of Precambrian Lode Gold Deposits and Implications for Exploration

Geology, hydrothermal alteration, and genesis of the world-class Canadian Malartic stockwork-disseminated Archean gold deposit, Abitibi, Quebec

Stéphane De Souza[1], Benoît Dubé[1], Vicki J. McNicoll[2], Céline Dupuis[1], Patrick Mercier-Langevin[1], Robert A. Creaser[3], and Ingrid M. Kjarsgaard[4]

[1]Geological Survey of Canada, Québec, Quebec
[2]Geological Survey of Canada, Ottawa, Ontario
[3]University of Alberta, Edmonton, Alberta
[4]Consulting Mineralogist, Ottawa, Ontario

2015

This publication is available for free download through GEOSCAN (http://geoscan.nrcan.gc.ca/)

Recommended citation

De Souza, S., Dubé, B., McNicoll, V.J., Dupuis, C., Mercier-Langevin, P., Creaser, R.A., and Kjarsgaard, I.M., 2015. Geology, hydrothermal alteration, and genesis of the world-class Canadian Malartic stockwork-disseminated Archean gold deposit, Abitibi, Quebec, *In:* Targeted Geoscience Initiative 4: Contributions to the Understanding of Precambrian Lode Gold Deposits and Implications for Exploration, (ed.) B. Dubé and P. Mercier-Langevin; Geological Survey of Canada, Open File 7852, p. 113–126.

Publications in this series have not been edited; they are released as submitted by the author.

Contribution to the Geological Survey of Canada's Targeted Geoscience Initiative 4 (TGI-4) Program (2010–2015)

TABLE OF CONTENTS

Geology, hydrothermal alteration, and genesis of the world-class Canadian Malartic stockwork-disseminated Archean gold deposit, Abitibi, Quebec

Stéphane De Souza[1]*, Benoît Dubé[1], Vicki J. McNicoll[2], Céline Dupuis[1], Patrick Mercier-Langevin[1], Robert A. Creaser[3], and Ingrid M. Kjarsgaard[4]

[1]Geological Survey of Canada, 490 rue de la Couronne, Québec, Quebec G1K 9A9
[2]Geological Survey of Canada, 601 Booth Street, Ottawa, Ontario, K1A 0E8
[3]Department of Earth and Atmospheric Sciences, University of Alberta, Edmonton, Alberta T6G 2E3
[4]Consulting Mineralogist, 15 Scotia Place, Ottawa, Ontario K1S 0W2
*Corresponding author's e-mail: sdesouza@nrcan.gc.ca

ABSTRACT

The Canadian Malartic Mine consists of an Archean low-grade bulk tonnage gold deposit (reserves of 10.7 Moz Au @ 0.97 g/t) hosted by clastic metasedimentary rocks of the Pontiac Group and subalkaline porphyritic quartz monzodiorite and granodiorite located immediately south of the Larder Lake–Cadillac Fault Zone. The quartz monzodiorite and granodiorite yield syn-Timiskaming U-Pb zircon ages of 2677 and 2678 Ma, respectively. Gold mineralization is characterized by zones of quartz-carbonate vein stockwork and disseminated pyrite with a Au-Te-W-S-Bi-Ag±Pb±Mo metallic signature. These ore zones are dominantly oriented subparallel to the northwest-striking S_2 foliation and to the east-striking and south-dipping Sladen Fault, thus forming northwest-southeast and east-west mineralized trends. Molybdenite from high-grade ore yielded a Re-Os age of ca. 2664 Ma. In both the sedimentary rocks and the quartz monzodiorite, the proximal and distal alteration zones are characterized by the presence of calcite and ferroan dolomite, respectively. In the sedimentary rocks, the ore zones show a wide distal biotite alteration halo with proximal assemblages comprising albite and/or microcline. The quartz monzodiorite comprises a distal hematitic alteration zone that is overprinted by proximal microcline + albite + quartz replacement zones. This study suggests that at Canadian Malartic deposit, the gold mineralization and its distribution are largely controlled by D_2 faults, shear and high-strain zones developed in the hinge zone of F_2 folds, and by the Sladen Fault. A ≤2678 Ma syn-Timiskaming magmatic-hydrothermal early phase of gold mineralization can be inferred by the metallic signature or the ore, the presence of mineralized stockworks, the potassic alteration (biotite/microcline), and association with porphyritic intrusions. The main characteristics of the Canadian Malartic deposit is thus best explained by syn-D_2 deformation gold (ca. 2670–2660 Ma) superimposed onto, or remobilized from, a gold-bearing magmatic/hydrothermal system related to Timiskaming-age porphyritic intrusions emplaced along a major fertile fault zone.

INTRODUCTION

The Canadian Malartic open pit mine consists of an Archean low-grade bulk tonnage gold deposit (10.7 Moz Au, in 343.7 Mt @ 0.97 g/t Au; Belzile and Gignac, 2011) located in the Malartic mining district in the Abitibi region of Quebec (Figs. 1 and 2). The open pit mine was put into production in 2011 and is being developed on the grounds of three past-producing underground mines that exploited the same auriferous hydrothermal system but at average ore grades varying between 3.3 and 4.9 g/t (Trudel and Sauvé, 1992). The Canadian Malartic gold deposit is characterized by the presence of disseminated and stockwork mineralization, along with vein-hosted gold in turbiditic metasedimentary rocks and porphyritic intrusions (Sansfaçon and Hubert, 1990; Trudel and Sauvé, 1992; Helt et al., 2014; De Souza et al., in press). In the Abitibi greenstone belt, stockwork and disseminated sulphide mineralization are common features of Archean Au and Au-Cu deposits associated with, and/or hosted by Timiskaming-age (2680–2672 Ma) quartz-feldspar porphyry (Robert, 2001). Such deposits have been interpreted either as genetically related to the porphyritic intrusive host rocks (Sinclair, 1982; Robert, 2001; Helt et al., 2014), or as structurally controlled

De Souza, S., Dubé, B., McNicoll, V.J., Dupuis, C., Mercier-Langevin, P., Creaser, R.A., and Kjarsgaard, I.M., 2015. Geology, hydrothermal alteration, and genesis of the world-class Canadian Malartic stockwork-disseminated Archean gold deposit, Abitibi, Quebec, *In:* Targeted Geoscience Initiative 4: Contributions to the Understanding of Precambrian Lode Gold Deposits and Implications for Exploration, (ed.) B. Dubé and P. Mercier-Langevin; Geological Survey of Canada, Open File 7852, p. 113–126.

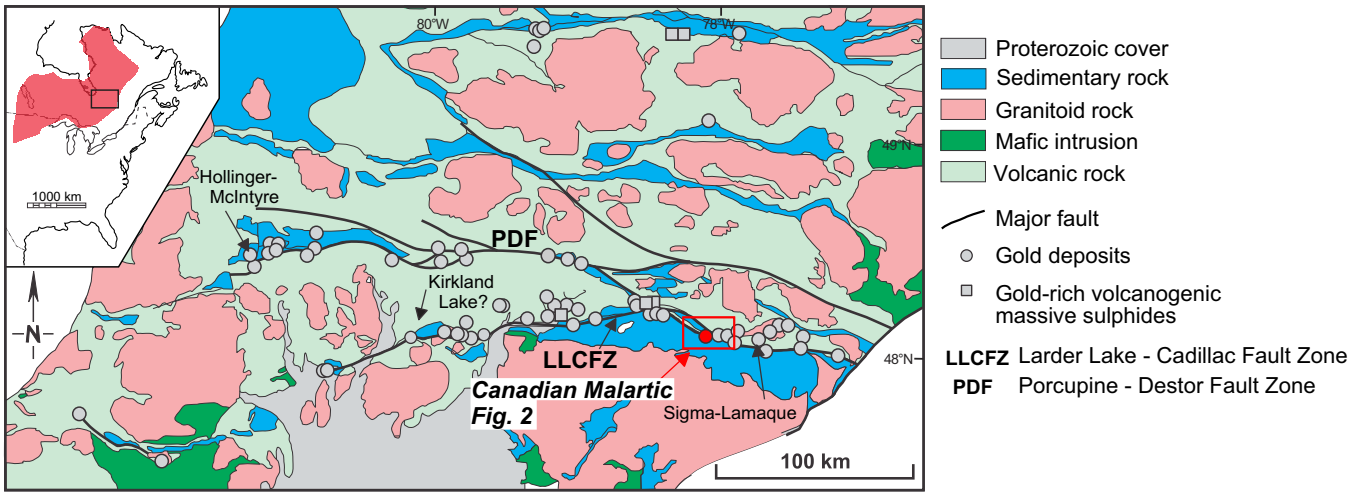

Figure 1. Simplified geological map of the Abitibi greenstone belt. Inset shows the location of the Superior Province. Adapted from Dubé and Gosselin (2007) and Poulson et al. (2000).

and, at least in part, contemporaneous with the main phase of deformation (Sansfaçon and Hubert, 1990; Trudel and Sauvé, 1992; Fallara et al., 2000; De Souza et al., 2013, in press; Zhang et al., 2014). At the Canadian Malartic Mine, calculated oxygen and hydrogen isotopic composition studies led to contrasting hypotheses on the origin of the Au mineralizing hydrothermal fluids, which are currently interpreted either as of magmatic (Helt et al., 2014) or metamorphic (Beaudoin and Raskevicius, 2014) origin. In this context, one of the main objectives of this project is to understand the geological parameters that control the distribution, genesis, and geological footprint of intrusion-associated gold deposits in deformed and metamorphosed Archean terranes.

The Canadian Malartic gold deposit is located within (Barnat zone) and immediately to the south (Canadian Malartic, Sladen and East Malartic zones) of the Larder Lake-Cadillac Fault Zone, which delineates the contact between the Abitibi Subprovince to the north and the Pontiac Subprovince to the south (Fig. 2). The fault zone is marked by volcanic and plutonic

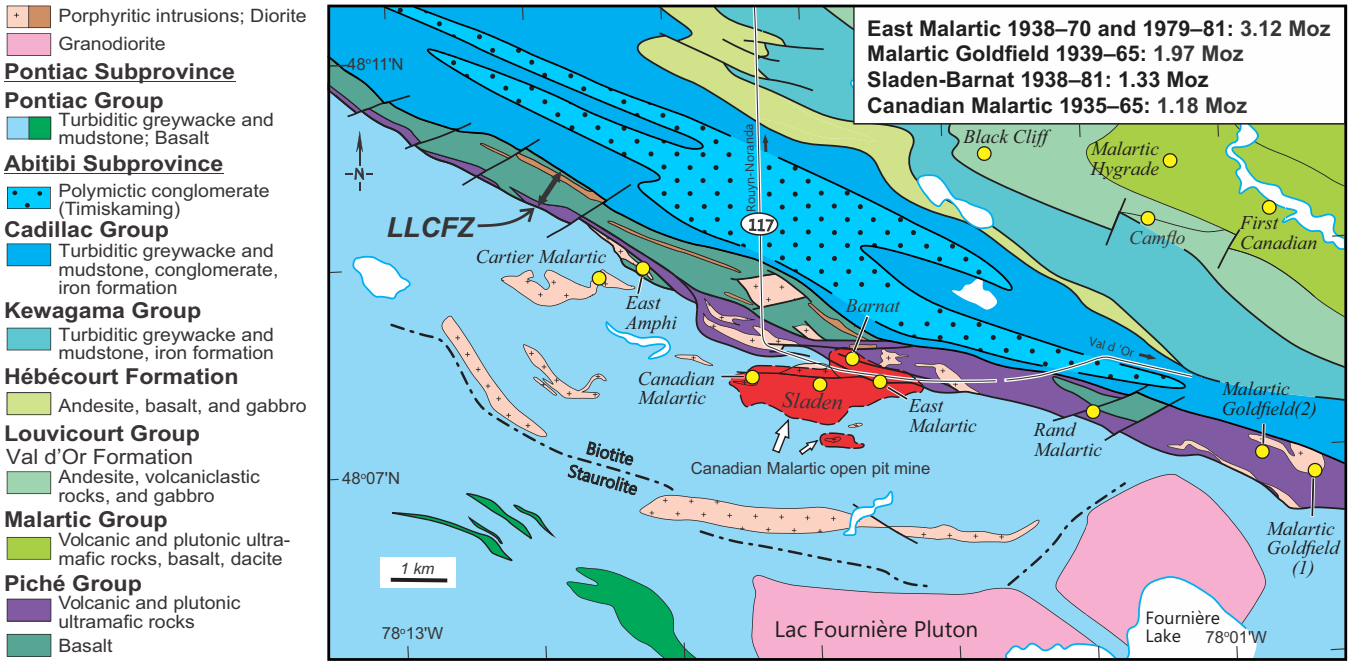

Figure 2. Geological map of the Malartic district showing the main past-producing gold mines and gold showings (yellow dots). The dash-dotted line corresponds to the staurolite isograd in the Pontiac Group sedimentary rocks. Geology is from this study and from Sansfaçon and Hubert (1990), Fallara et al. (2005), Grant et al. (2005), Pilote (2013), and Pilote et al. (2014). The final expected configuration of the Canadian Malartic open pit mine is shown in red. The gold production data for the past-producing East Malartic, Sladen-Barnat, Canadian Malartic, and Malartic Gold Fields are from Trudel and Sauvé (1992). LLCFZ: Larder Lake – Cadillac Fault Zone.

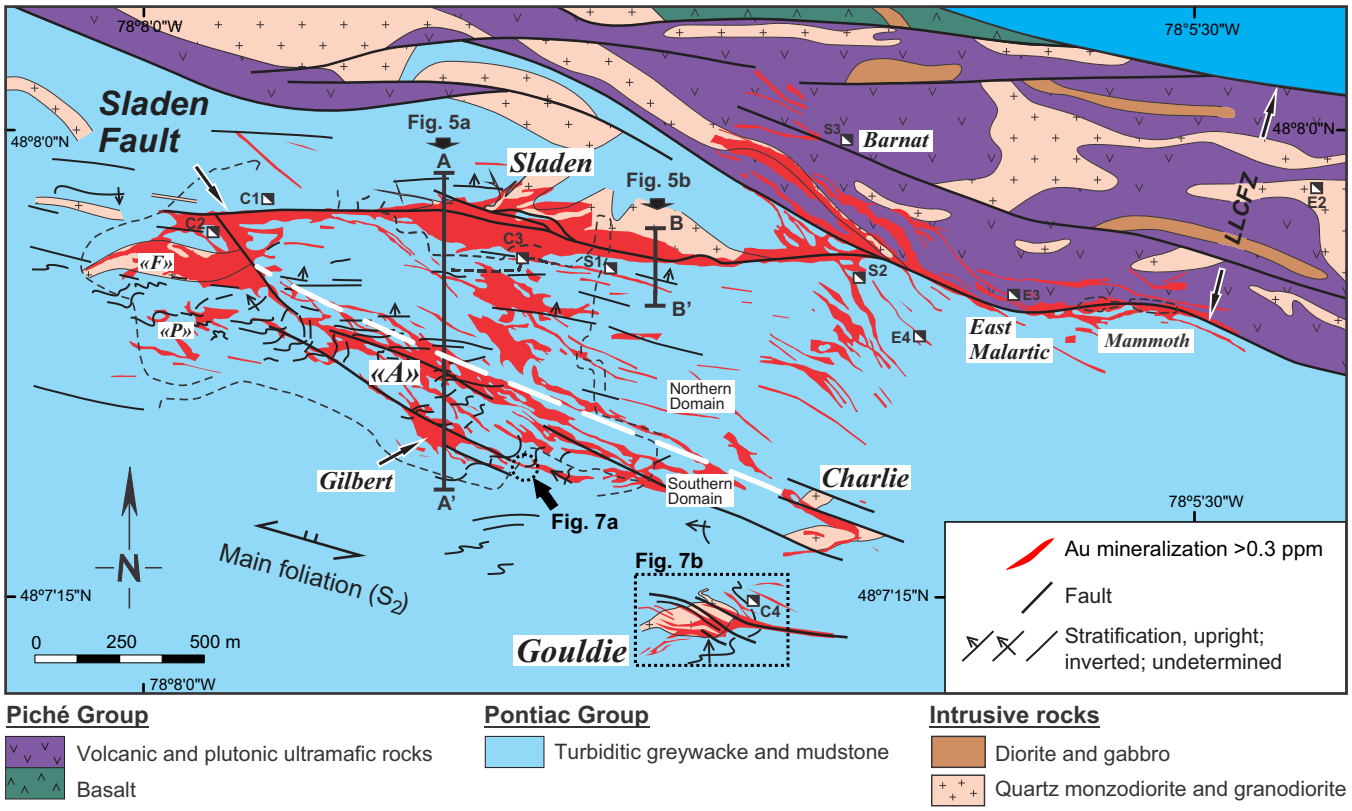

Figure 3. Geological map of the Canadian Malartic open pit gold mine. Geology from this study and from Derry (1939), Sansfaçon and Hubert (1990), and Fallara et al. (2000). Mineralized zones (≥0.3 g/t Au) are shown in red. The outline of the open pit mine, as of September 2012, is shown as a dashed line. The approximate limit between the northern and southern structural domains is identified by a white dashed line. Names of the main mineralized ore zones are identified in italic font. Location of the shafts of the past-producing mines: C = Canadian Malartic, E = East Malartic, S = Sladen-Barnat.

mafic-ultramafic rocks of the Piché Group (Fig. 2; Card, 1990; Daigneault et al., 2002). As in the Kirkland Lake and Timmins districts, Timiskaming-age polymictic conglomerate units have been recently identified immediately to the north of the Larder Lake-Cadillac Fault Zone and were dated at <2676 and 2678 Ma by Pilote et al. (2014). The Canadian Malartic gold deposit is mostly hosted by turbiditic greywacke and mudrock of the Pontiac Group (ca. 2685–2682; Davis, 2002) and by Timiskaming-age, ca. 2677–2678 Ma, porphyritic quartz monzodiorite to granodiorite intrusions (Helt et al., 2014; De Souza et al., in press). The metamorphic grade increases rapidly southward in the Pontiac Group (Sansfaçon and Hubert, 1990; Benn et al., 1994), from the biotite-chlorite zone along the southern contact of the Larder Lake-Cadillac Fault Zone, to garnet and staurolite zones within about 2 km to the south (Fig. 2). In the Malartic district, structural studies have shown that the Pontiac Group has undergone polyphase deformation and comprises a northeast-trending bedding-parallel S_1 foliation overprinted by a northwest-striking S_2 cleavage that represents the dominant foliation in the mine area (Sansfaçon and Hubert, 1990; Desrochers and Hubert, 1996; De Souza et al., in press).

GEOLOGY OF THE CANADIAN MALARTIC GOLD DEPOSIT

The Canadian Malartic open pit mine is mainly hosted by sedimentary rocks of the Pontiac Group (~70%; Fig. 3), which show a metamorphic paragenesis that comprises biotite, muscovite, oligoclase, chlorite, and epidote. Pyrite, pyrrhotite, ilmenite, magnetite, monazite and apatite are also present in variable proportions. These rocks are relatively weakly strained and show well preserved sedimentary structures. Sixty-five individual detrital zircon grains were collected from a sample of coarse-grained greywacke. The youngest U-Pb dating of which suggests a maximum age of ca. 2685 Ma (De Souza et al., in press), an age constraint similar to the one obtained by Davis (2002).

At the mine site, sedimentary rocks of the Pontiac Group are cut by dykes and sills of various compositions, all of which are known to show some evidence of hydrothermal alteration and to host, at least locally, ore-grade gold mineralization. These intrusive rocks include porphyritic quartz monzodiorite and granodiorite, intermediate and felsic dykes, and widespread lamprophyre dykes.

The quartz monzodiorite is mostly located in the

northern and western parts of the deposit and represents the main mineralized intrusive phase in the mine (Fig. 3). It is magnetite- and titanite-bearing and consists of perthitic orthoclase phenocrysts embedded within an equigranular groundmass composed of plagioclase, biotite, hornblende, epidote, quartz, and muscovite, with minor apatite, zircon, and ilmenite (Fig. 4a). The quartz monzodiorite can further be divided into low- and high-TiO_2 subtypes that are characterized by average TiO_2 values of ~0.34 and ~0.49 wt%, respectively. The low-TiO_2 subtype has normative compositions intermediate between quartz monzodiorite and granodiorite, but is referred to as quartz monzodiorite throughout the text. The porphyritic granodiorite is mostly present at the Gouldie zone (Fig. 3) and consists of 4 mm to 1 cm perthite phenocrysts that are set in an equigranular groundmass of quartz, plagioclase, muscovite, biotite, microcline, apatite, epidote, titanite, and pyrite. Molybdenite is locally present in the porphyritic granodiorite as disseminated flakes in the igneous groundmass, in "blue" quartz veins, or in molybdenite-pyrite-quartz veins.

Several samples of intrusive rocks were collected for U-Pb geochronology. The porphyritic quartz monzodiorite has yielded zircon and titanite ages of 2677 Ma and 2676 Ma, respectively, whereas zircons from the Gouldie zone granodiorite were dated at 2678 Ma. One felsic dyke from the open pit has yielded a zircon age of 2677 Ma. Thus, despite differences in composition of the intrusive rocks, geochronological studies indicate that the magmatic event(s) centred in the Malartic area happened in a restricted syn-Timiskaming 2678–2676 Ma time interval.

Structural Setting

In the mine area, S_2 is generally northwest-trending, northeast-dipping (65–90º) and is axial planar to F_2 open to closed folds that plunge steeply toward the east (Fig. 4b). F_2 folds form antiformal syncline and synformal anticline pairs, which are interpreted as the result of refolding of F_1 overturned folds. The S_1 foliation is only locally preserved in F_2 fold hinge zones and consists of a folded penetrative schistosity marked by white mica. The mine area has been divided into northern and southern structural domains based on the orientation of bedding relative to the S_2 cleavage (Fig. 3). The southern and northern domains represent the hinge zone and the long limb of a mine-scale S-type F_2 fold, respectively. Figure 5a also illustrates the distribution and geometry of the ore zones relative to the main structural features and host rocks. The east-trending Sladen Fault dips moderately to steeply (45–80º) toward the south and intersects the Piché Group in the eastern part of the deposit, where it is interpreted to locally mark the southern limit of the Larder Lake-Cadillac Fault Zone (Sansfaçon and Hubert, 1990). The Sladen Fault varies from a ~10 m-wide planar brittle±ductile deformation and alteration zone, to a ~100 m-wide fault zone comprising multiple subsidiary faults with evidence of both ductile and brittle strain increments. Banded porphyroclastic mylonite facies are present but discontinuous along and within ≤3 m into the footwall of the Sladen Fault, in the quartz monzodiorite. Hydrothermally altered fault breccia is also locally present, mostly in the quartz monzodiorite, and quartz breccia veins are common along the main fault segments in the sedimentary rocks. Cataclasite is locally superimposed on deformed and altered rocks and a 10 cm- to 2 m-wide zone of brittle deformation containing fault gouge, brecciated rock, and dismembered quartz veins generally marks a late fault plane.

Mineralization, Alteration, and Re-Os Dating

In the Canadian Malartic deposit, gold occurs mostly as <20 µm free gold grains and inclusions in pyrite, which are distributed in stockworks and veins (Fig. 4c) as well as disseminated in the altered host rocks (Fig. 4d). Gold is associated with trace amounts of Te-W-Bi±Ag and locally Mo±Pb (De Souza et al., in press). The mineralization is distributed according to two main trends forming east-west and northwest-southeast ore zones (Fig. 3). At the surface, the dominant east-west trace of the Sladen ore zone coincides with the position of the Sladen Fault and gold is hosted by quartz monzodiorite and by sedimentary rocks along and adjacent to the fault (Fig. 5). The surface trace of the northwest-southeast mineralized trend is subparallel to the S_2 cleavage. These northwest-trending ore zones dip steeply to moderately toward the northeast and are mainly hosted by sedimentary rocks and local dykes or sills. Mineralized rocks contain up to 5% disseminated pyrite with trace amounts of chalcopyrite, galena, scheelite, and telluride minerals. Molybdenite and sphalerite are locally present. Molybdenite from sedimentary rock-hosted high-grade gold mineralization was selected for Re-Os dating and yielded an age of ca. 2664 Ma.

Au-Related Veins

Among the different vein types documented during this study, three are closely related to auriferous hydrothermal alteration, and are present in the sedimentary rocks and in the quartz monzodiorite (V_1, V_2, and V_3 veins). The V_4 and V_5 veins are barren and post-date mineralization.

The V_1 veins are 1 mm to 3 cm in width, have low gold values (9 ppb to 0.44 ppm Au), and pre-date the main ore-forming stage. They are mainly composed of quartz with minor amounts of pyrite, albite, calcite, galena, molybdenite, biotite, and chlorite. The V_2 veins are related to the main stage of gold mineralization and

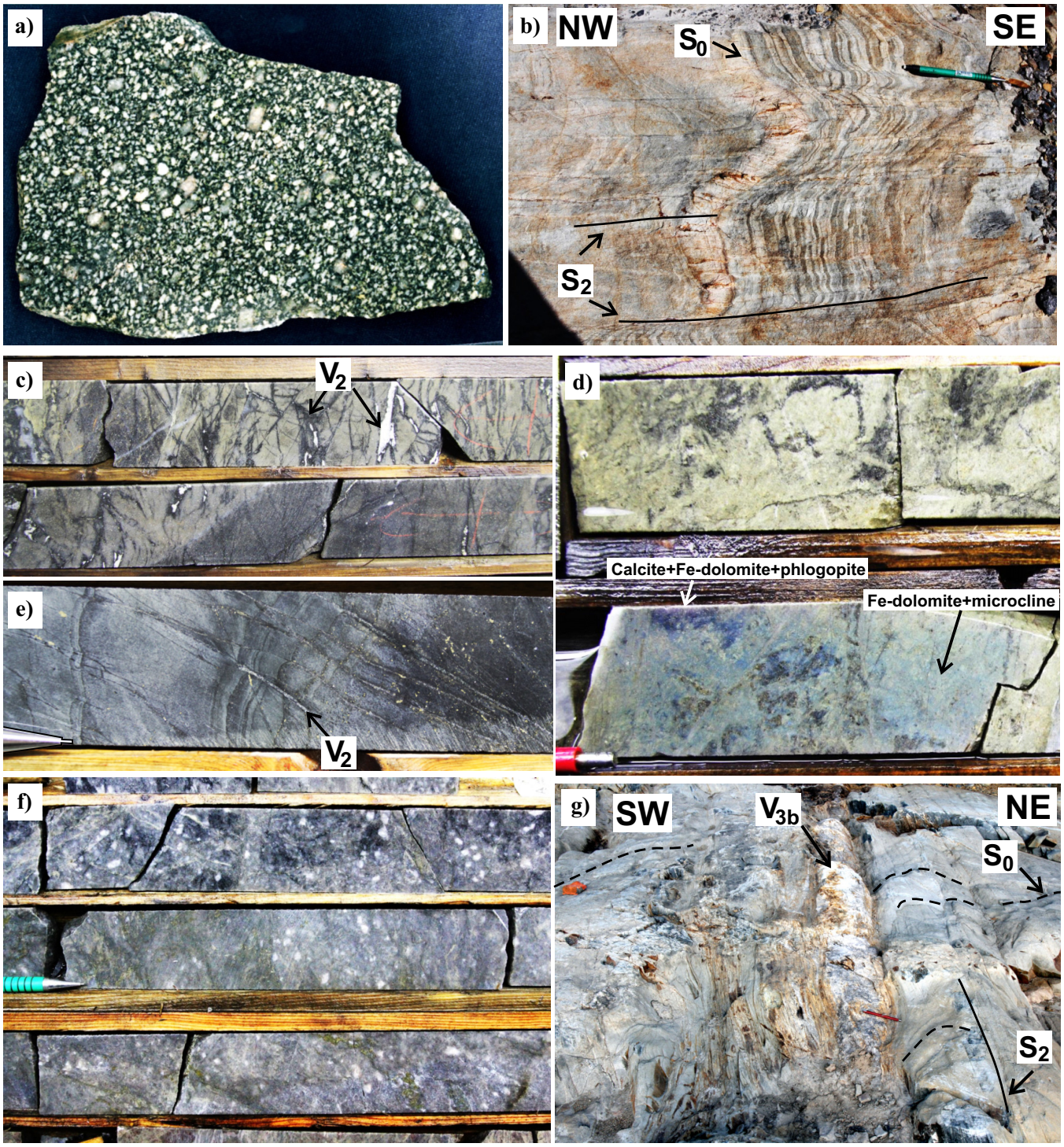

Figure 4. Field photographs. **a)** Least-altered quartz monzodiorite of the Sladen zone. **b)** F_2 folds in massive to laminated greywacke and mudstone of the Pontiac Group showing S_2 pressure-solution cleavage. Younging direction is to the northwest. **c)** Stockwork of V_2 veinlets and disseminated gold mineralization in altered greywacke. **d)** Proximal alteration in greywacke with ferroan dolomite coloured blue using carbonated staining technics. Notice the local presence of calcite (pinkish/purple) in biotite-rich zones. **e)** V_2 quartz veinlets with biotite-rich pyritized selvages in a distal alteration zone in sedimentary rocks. Veinlets are formed perpendicular to bedding. **f)** Proximal alteration zone in quartz monzodiorite, footwall of the Sladen Fault. **g)** High-grade laminated V_{3b} quartz vein in D_2 high-strain zone cutting the stratification at a high-angle. See Figure 7a for location.

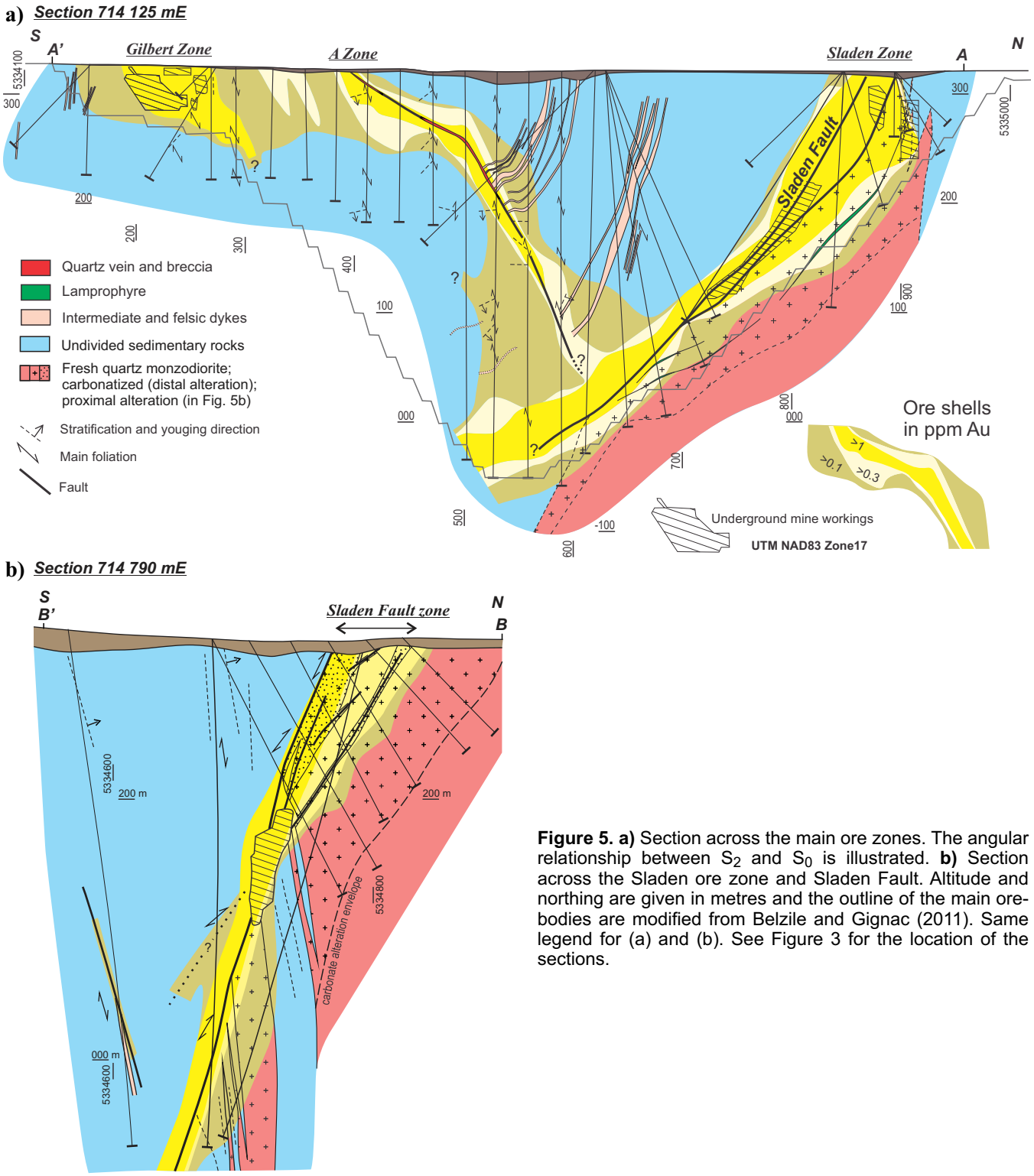

Figure 5. a) Section across the main ore zones. The angular relationship between S_2 and S_0 is illustrated. **b)** Section across the Sladen ore zone and Sladen Fault. Altitude and northing are given in metres and the outline of the main orebodies are modified from Belzile and Gignac (2011). Same legend for (a) and (b). See Figure 3 for the location of the sections.

are present in all rock types. These veins are 1 mm to 1 cm in width, generally show biotite selvages, and are composed of various proportions of quartz, calcite, ferroan dolomite, biotite, microcline, albite, chlorite, pyrite, and ankerite (Fig. 4c) with trace amounts of chalcopyrite, tellurides, gold, and scheelite. These V_2 veins occur as stockworks (Fig. 4c), as filled fractures and faults subparallel or at low-angle relative to the S_2 cleavage (Fig. 4e), or in some cases as crenulated veinlets at high-angle to S_2. The presence of deformed and undeformed V_2 veinlets suggests that they were emplaced syn- to late-D_2.

The V_3 veins cut V_2 veins and can be divided into three distinct subtypes: V_{3a}, V_{3b}, and V_c. The V_{3a}

veins are discontinuous, have well to poorly defined margins and in some cases are related to silica flooding of the host rocks. The V_{3a} veins consist of fine-grained white to grey saccharoidal quartz with finely disseminated pyrite and locally abundant molybdenite. The V_{3b} quartz-pyrite±galena veins are known to host high-grade Au values of up to 42.3 ppm. They form 1 cm- to 2 m-thick fault-fill laminated and breccia veins. The V_{3c} veins are mostly present in the quartz monzodiorite and granodiorite, and form 1 cm- to 30 cm-wide extensional veins that are dominated by quartz with variable proportions of coarse albite, muscovite, ankerite, calcite, biotite, pyrite, chlorite, and minor amounts of hematite, rutile, K-feldspar, tourmaline, galena, scheelite, native free gold, tellurides, and chalcopyrite. Derry (1939) described these veins as "pegmatitic", since grain size can reach up to 5 cm. Our analyses of such V_{3c} veins have yielded gold values of 0.013 to 6.7 ppm.

Distal and Proximal Hydrothermal Alteration Assemblages

Both the sedimentary and intrusive rocks are characterized by distal and proximal hydrothermal alteration assemblages with mineral compositions that are strongly influenced by the composition of the protolith. The main types of alteration that were documented are widespread carbonate alteration (calcite + ferroan dolomite ± ankerite) and sulphidation of the sedimentary and intrusive rocks. Biotite and K-feldspar potassic alteration is also important, whereas albitization and silicification are mostly developed in the sedimentary and intrusive rocks, respectively. Distal alteration zones are in excess of ~150 m. The proximal alteration haloes are up to 30 m wide, but larger zones containing almost continuous stockwork and/or proximal replacement zones over 70 m have also been documented.

In the sedimentary rocks, distal assemblages are composed of biotite, white mica, plagioclase, with minor amounts of pyrite and calcite (Fig. 4e). The carbonate and pyrite contents increase toward proximal alteration and ore zones. Carbonate minerals are mostly present in the greywacke facies and are almost absent from mudstone. The proximal assemblage in the sedimentary rocks is light beige and composed of fine-grained (5–20 um) albite and/or microcline with ferroan dolomite, calcite, quartz, phlogopite, and minor white mica (Fig. 4d). Phlogopite is F-rich (0.2–1.4 wt% F) and is absent from pervasively altered sedimentary rocks. Both the distal and proximal assemblages occur within D_2 high-strain zones, as replacement-style alteration controlled by protolith composition, and as selvages to V_2 and V_{3a-b} veins.

In the quartz monzodiorite, distal and proximal alteration assemblages are best developed in the high-TiO_2 subtype. The distal assemblage consists of a dark grey to reddish facies comprising calcite, hematite, biotite, and microcline, as well as magnetite, pyrite, chlorite, and rutile pseudomorphs after titanite and ilmenite. The proximal alteration consists of grey to pinkish (± hematite) microcline, albite, quartz, ferroan dolomite, rutile ± calcite assemblages that vary from vein selvages to a pervasive hydrothermal replacement (Fig. 4f). A fine-grained cherty subtype of the proximal grey alteration shows relict feldspar phenocrysts obscured by alteration, recrystallization, and by the local development of a mylonitic fabric.

At the Gouldie zone, hydrothermal alteration of the granodiorite is widespread and largely controlled by the presence of sheeted V_3 quartz veins and stockworks, whereas fresh granodiorite is seldom preserved. The dominant alteration facies is greenish to white-coloured and represented by a mineral assemblage consisting of calcite, ferroan dolomite, white mica, albite, microcline, quartz, pyrite and rutile. V_3 veins often show bleached selvages that are mainly composed of feldspar, quartz, and carbonate. Although in trace amounts overall, molybdenite is locally abundant in quartz veins, disseminated in the altered granodiorite, or as coating fractures.

Mass gain/loss in K_2O, Na_2O, and SiO_2 was calculated according to the isocon method of Grant (1986) for a set of samples collected from surface outcrops of the Sladen zone distributed ~150 m to the west and east of the section shown in Figure 5b. In the footwall of the Sladen Fault, the distal alteration assemblage hosted by the quartz monzodiorite shows negligible Na_2O variation and low K_2O increase of approximately 0 to +45 wt% related to variable Au values of <0.005 to 1.25 ppm. In the immediate footwall of the Sladen Fault, the proximal alteration assemblage shows marked increases in K_2O (+80 to +360 wt%) and SiO_2 (+30 to +250 wt%) and leaching of Na_2O (-2 to -80 wt%). In the sampled area, intense alteration of sedimentary rocks is mostly restricted to ca. 2 m within the hanging wall of the Sladen Fault, where sedimentary rocks are characterized by strong Na_2O enrichment (+40 to +330 wt%) and K_2O leaching in proximal altered zones (-15 to -40 wt%). Molar CO_2/CaO and CO_2/(CaO+MgO) ratios for these same samples suggest that, irrespective of the host rock type, ore-grade gold values (i.e. ≥0.30 ppm) are present in the samples with strongest carbonatization (molCO_2/(molCaO) >0.8; Fig. 6a), and that the wt% CO_2 content is largely dependent on the nature of the protolith and its capacity to react with the gold-bearing CO_2-rich fluid (Fig. 6b; e.g. Davies et al., 1982, 1990).

Characteristics of the Northwest-Southeast- and East-West-Trending Ore Zones

Northwest-southeast-trending ore zones include the P,

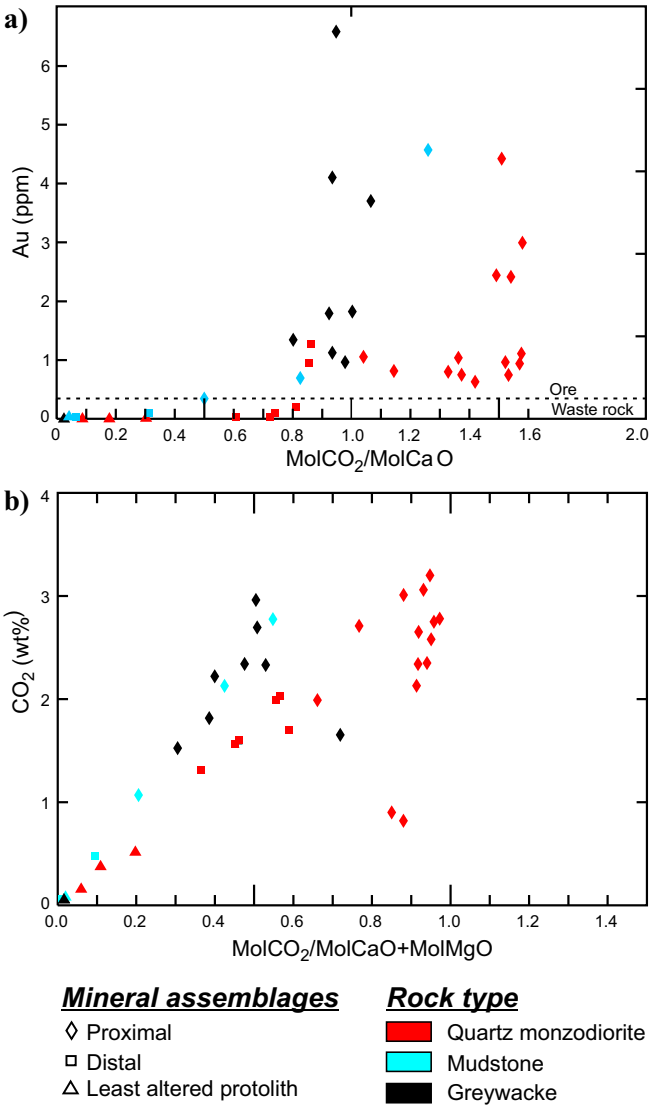

Figure 6. a) Au (ppm) vs molar CO_2/CaO ratio and **(b)** CO_2 wt% vs. molar CO_2/(CaO+MgO) diagrams for samples of greywacke, mudstone, and quartz monzodiorite from the Sladen ore zone.

A, Gouldie, and Gilbert zones, which show relatively similar alteration types and are discordant relative to bedding and to intrusive rocks. The P zone is, however, partly stratabound and controlled by the geometry of the folded strata (e.g. Sansfaçon et al., 1987). The Gilbert and A zones are subparallel, dip northward, and represent the main northwest-southeast-trending ore zones.

In the Gilbert zone, auriferous alteration zones are distributed in a series of subparallel, planar north-northeast-dipping D_2 high-strain zones varying from 5 cm to 3 m wide and developed at a high-angle to the folded bedding and felsic feldspar-phyric sill-like intrusions (Fig. 7a). The high-strain zones show closed to locally tight fold hinges that are dismembered by sets of parallel brittle faults filled by V_2 veinlets. Auriferous V_{3b} veins are present in some of the high-strain zones and yield up to 33.4 ppm Au (Fig. 4g). Distal and proximal alteration assemblages are present in the Gilbert zone as selvages of the V_2 veinlets and within high-strain zones, with gold values up to 6.11 ppm. The porphyritic felsic sill yields low gold values (<0.3 ppm) and shows minor carbonatization and sulphidation (mainly pyrite). An east-northeast-plunging mineral lineation with a steep pitch (~60–80º) is locally marked by biotite and by quartz fibres in V_{3b} veins (Fig. 7a). Kinematic indicators are scarce in the high-strain zones, but the dragging and displacement of the faulted dykes, together with the local occurrence of back-rotated quartz-vein boudins suggest a dominant top-to-the-southwest reverse sense of shear.

As shown in Figure 5a, the A-zone is centred on a D_2 fault zone that hosts V_{3a} and V_{3b} veins and clearly cuts south-dipping to subvertical dykes in the Pontiac Group. This fault zone also coincides with the transition from the northern to the southern structural domains. From the surface down to a depth of approximately 100 m, the A zone is marked by a sharp inflexion from a shallow to a steep dip. Considering the interpreted reverse sense of motion along D_2 faults, this inflexion can be interpreted as a dilational bend/jog structure or relay zone that may have acted as a preferential lower pressure fluid pathway during mineralization.

At the Gouldie zone, gold is distributed along and parallel to a north-dipping, west-northwest-trending, approximately ≤5- to 8-m-wide, D_2 high-strain zone formed at high-angle to the bedding in a F_2 hinge zone (Fig. 7b). This mineralized zone is continuous for >500 m along-strike toward the east-southeast and intersects a porphyritic granodiorite intrusion at its northwestern extremity. In the sedimentary rocks, the Gouldie zone shows typical alteration zonation with light-coloured proximal alteration and disseminated pyrite associated with V_2 veinlets and V_{3b} veins. However, V_{3b} veins are extensive and are locally up to 2 m wide. Detailed mapping has also revealed that D_2 faults and shear zones follow lamprophyre dykes, possibly due to competency contrasts between the dykes and the host rocks (Fig. 7b). The steep to moderate pitch (55–75º) of the northeast-plunging mineral lineation in the high-stain zone and the geometry of the quartz fibres in the quartz veins suggest a reverse sense of shear with a sinistral slip component (De Souza et al., in press).

Along east-west-trending ore zones, the quartz monzodiorite to the north of the Sladen Fault is strongly altered to proximal assemblages along the main fault segments. The distal alteration assemblage is developed as an alteration halo up to 100 m into the footwall of the Sladen Fault (Fig. 5b) and as selvages of V_1 veins. The main Sladen ore zone dips steeply to the south but westward it becomes shallow dipping at depth.

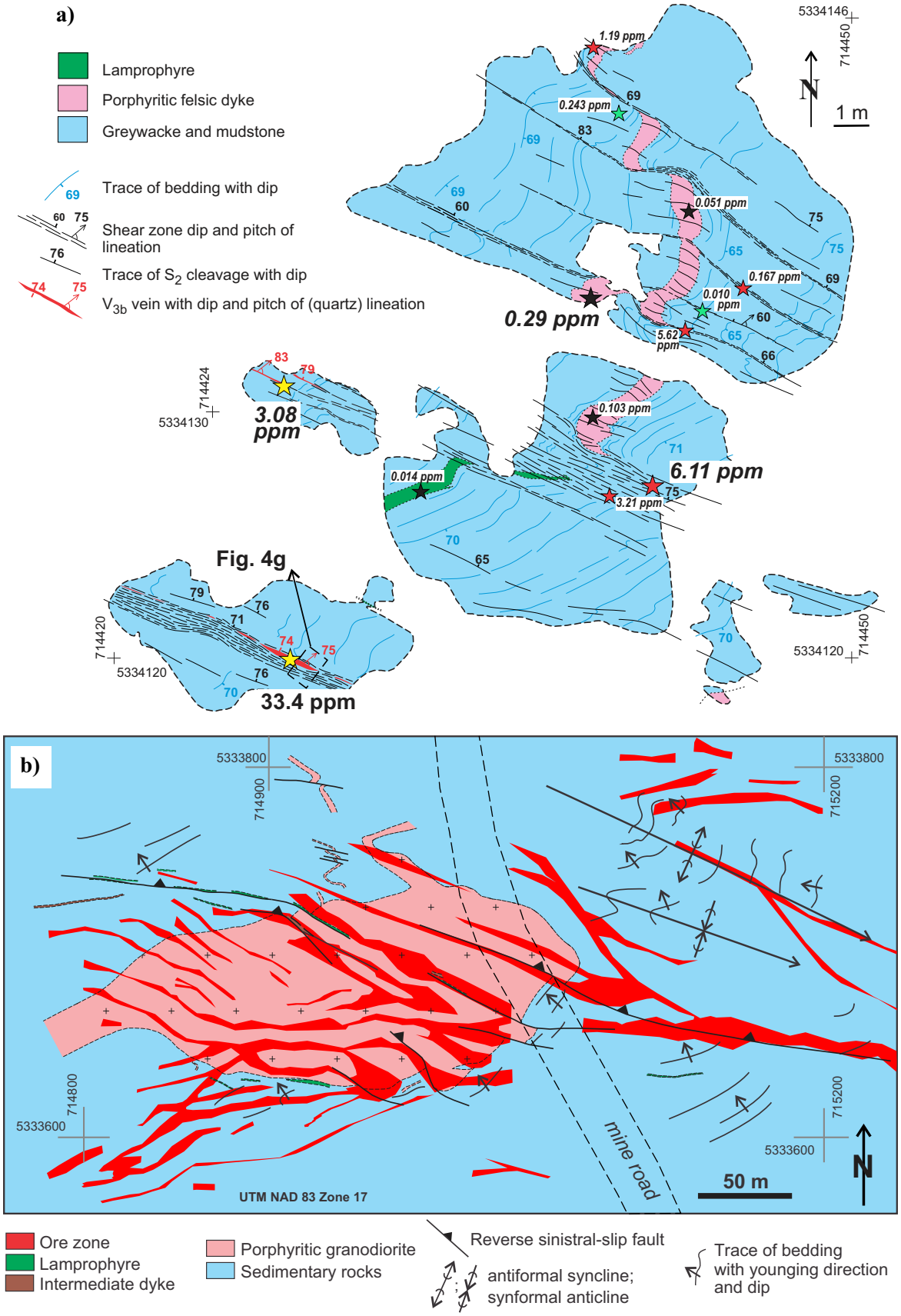

Figure 7. a) Detailed outcrop map of the southeastern extension of the Gilbert zone. Green, red, black, and yellow stars indicate the location and gold content of assayed samples of distal alteration, proximal alteration, dyke-hosted mineralization, and V_{3b} vein, respectively. **b)** Geological map of the Gouldie zone. See Figure 3 for locations.

DISCUSSION OF GENETIC MODELS

Compiled U-Pb ages and data presented herein clearly indicate that Timiskaming-age 2677–2678 Ma quartz monzodiorite and granodiorite, which host part of the mineralization at the Canadian Malartic Mine, were intruded into the Pontiac Group (ca. 2685–2682 Ma) metasedimentary rocks prior to D_2 main phase deformation and metamorphism in the southern Abitibi Subprovince (i.e. 2670–2660 Ma; Ayer et al., 2005; Robert et al., 2005, and references therein). An early magmatic-hydrothermal gold mineralization event, as originally proposed by Issigonis (1980), can be inferred based on the presence of widespread potassic alteration (microcline and biotite), the Au-Te-W-Bi±Ag±Mo±Pb metallic signature of the ore (e.g. Goldfarb et al., 2005; Hart, 2007), and by the spatial association of mineralization with porphyritic intrusions. Moreover, the Canadian Malartic deposit shares analogies with the structurally controlled sedimentary rock-hosted intrusion-related deposits, as described by Robert et al. (2007), especially in terms of host rock, metallic signature and alteration (feldspar, sericite, carbonate and biotite), but also because such deposits are commonly located in the core of anticlines cut by high-angle faults in proximity to a crustal scale fault. However, a simple magmatic-hydrothermal model at Canadian Malartic cannot entirely explain the northwest-southeast and east-west distribution of the ore zones, nor the interpreted chronology of mineralization relative to deformation and magmatism. Field evidence suggests that at least part of the alteration assemblages, disseminated orebodies, and vein networks are associated with widespread brittle and brittle-ductile structures formed as a result of D_2 deformation. V_2 veins emplaced along the S_2 cleavage and fractures/faults axial planar to F_2 folds, together with the presence of quartz veins (V_{3a} and V_{3c}), filling fractures, and faults at high angle to folded bedding, are indicative of gold-bearing hydrothermal fluids invading D_2 structures. A syndeformation stage of gold mineralization is also compatible with the ca. 2664 Ma Re-Os molybdenite age, which overlaps with the inferred age of the regional main phase D_2 deformation as well as with the bulk of lode gold mineralization (2670–2660 Ma) in the southern Abitibi (e.g. Ayer et al., 2005; Robert et al., 2005; Dubé and Gosselin, 2007). The D_2 deformation model is compatible with the widespread carbonate alteration that typifies a large number of gold deposits along the Larder Lake-Cadillac and Destor-Porcupine fault zones in the Abitibi greenstone belt (e.g. Dubé and Gosselin, 2007 and references therein). The main characteristics of the Canadian Malartic deposit are thus best explained by syn-D_2 deformation gold (ca. 2670–2660 Ma) superimposed onto, or partly remobilized from, an early gold-bearing magmatic/hydrothermal system related to Timiskaming-age porphyritic intrusions emplaced along a major fertile fault zone. Moreover, aside from the gold being mostly hosted by turbiditic clastic sedimentary rocks, the Malartic deposit exhibits several common features of Archean orogenic gold deposits (cf. Goldfarb et al., 2005), including a combination of widespread carbonate alteration, overall low Cu, Bi, Zn and Pb contents, CO_2, K_2O, Na_2O, and S hydrothermal metasomatism, and the spatial association with brittle-ductile faults and shear zones. Also, as illustrated by the distribution of the orebodies and the underground workings of the past-producing mines, the Sladen Fault has played a major role in the formation of the Canadian Malartic deposit, and represents one of the main conduits for the rising gold-bearing hydrothermal fluid(s). The close relationship between mineralization and a brittle fault next to the Larder Lake-Cadillac Fault Zone, as well as the association with calc-alkaline porphyritic intrusions emplaced in sedimentary rocks, the hydrothermal carbonate alteration and the positive correlation between Au and Te are similar to key features of the giant syenite-hosted Kirkland Lake gold deposit located further west along the Larder Lake-Cadillac Fault Zone (e.g. Ispolatov et al., 2008 and references therein).

IMPLICATIONS FOR EXPLORATION

As it is the case for the Canadian Malartic deposit and for most greenstone-hosted lode gold deposits, the proximity to a major fault and the association of porphyritic intrusions, carbonatized mafic to ultramafic rocks, and Timiskaming-like fluvial/alluvial sedimentary rocks are key geological parameters for the formation and preservation of major deposits (Poulsen et al., 1992; Hodgson, 1993; Goldfarb et al., 2005; Robert et al. 2005; Dubé and Gosselin, 2007; Bleeker, 2012). The identification of such key geological parameters is thus of major importance in exploration targeting. The lack of known gold mineralization more than ~2–3 km south of the Pontiac-Piché contact, which also corresponds to the transition from biotite zone metamorphism and brittle to brittle-ductile deformation, to higher grade garnet and staurolite zone metamorphism and dominantly ductile deformation, may also help to underline prospective gold corridors south of the Larder Lake-Cadillac Fault Zone. In this context, the Sladen Fault and brittle-ductile D_2 faults formed in fold hinges and along short limbs of drag folds, have proven to represent fertile hydrothermal conduits for the circulation of gold-bearing fluids. Alteration haloes in excess of 150 m that include a distal assemblage with calcite in variable amounts in both the sedimentary rocks and quartz monzodiorite, also provide useful vectors for exploration. The Au-Te-W-Bi±Ag metallic

signature of the ore and the potassic component of the alteration assemblages (biotite+muscovite and K-feldspar) are key features that can also be applied in geochemical prospecting.

ACKNOWLEDGEMENTS

This project is conducted in collaboration with P. Pilote and P. Roy of the Ministère de l'Énergie et des Ressources naturelles du Québec, and the Canada Mining and Innovation Council (CMIC) footprints project, including R. Linnen, G. Olivo, A. Galley, M. Lesher, F. Robert, A.E. Williams-Jones, and especially S. Perrouty, N. Gaillard, N. Piette-Lauzière, R. Enkin, N. Elgoumi, and C. Bérubé-Lafrenière, who are all gratefully acknowledged for collaborating in this joint project. Special thanks are also due to all of the Osisko and Mine Canadian Malartic exploration and production team. We are profoundly thankful to D. Gervais and F. Bouchard of the Mine Canadian Malartic partnership, and to R. Wares, P. de Chavigny, and L. Caron for sharing their knowledge of the Canadian Malartic deposit. S. Castonguay, S. Jackson, J.F. Gao, W. Bleeker, J. Moorehead, H.K. Poulsen, F. Robert, M. Bardoux, D. Sillitoe, D. Sinclair, J.-F. Couture, and J. Clark contributed to constructive discussions and are sincerely acknowledged.

REFERENCES

Ayer, J.A., Thurston, P.C., Bateman, R., Dubé, B., Gibson, H.L., Hamilton, M.A., Hathway, B., Hocker, S.M., Houlé, M.G., Hudak, G., Ispolatov, V.O., Lafrance, B., Lesher, C.M., MacDonald, P.J., Péloquin, A.S., Piercey, S.J., Reed, L.E., and Thompson, P.H., 2005. Overview of results from the Greenstone Architecture Project: Discover Abitibi Initiative; Ontario Geological Survey, Open File Report 6154, 146 p.

Belzile, E. and Gignac, L.P., 2011. Updated resource and reserve estimates for the Canadian Malartic project Malartic, Quebec; NI 43-101 Report, 261 p.

Beaudoin, G. and Raskevicius, T., 2014. Constraints on the genesis of the Archean oxidized, intrusion-related Canadian Malartic gold deposit, Quebec, Canada: A discussion; Economic Geology, v. 109, p. 2067–2068.

Benn, K., Miles, W., Ghassemi, M.R., and Gillett, J., 1994. Crustal structure and kinematic framework of the northwestern Pontiac Subprovince, Quebec: An integrated structural and geophysical study; Canadian Journal of Earth Sciences, v. 31, p. 271–281.

Bleeker, W., 2012. Targeted Geoscience Initiative 4: Lode gold deposits in ancient deformed and metamorphosed terranes: The role of extension in the formation of Timiskaming basins and large gold deposits, Abitibi greenstone belt – A discussion; Ontario Geological Survey, Open File Report 6280, p. 47-1 to 47-12.

Card, K.D., 1990. A review of the Superior Province of the Canadian Shield, a product of Archean accretion; Precambrian Research, v. 48, p. 99–156.

Daigneault, R., Mueller, W., and Chown, E.H., 2002. Oblique Archean subduction: Accretion and exhumation of an oceanic arc during dextral transpression, Southern Volcanic Zone, Abitibi Subprovince, Canada; Precambrian Research, v. 115, p. 261–290.

Davies, J.F., Whitehead, R.E.S., Cameron, R.A., and Duff, D., 1982. Regional and local patterns of CO_2-K-Rb-As alteration: A guide to gold in the Timmins area, *In:* Geology of Canadian Gold Deposits, (ed.) R.W. Hodder and W. Petruk; Canadian Institute of Mining and Metallurgy, Special Volume 24, p. 130–143.

Davies, J.F., Whitehead, R.E., Huang, J., and Nawaratne, S., 1990. A comparison of progressive hydrothermal carbonate alteration in Archean metabasalts and metaperidotites; Mineralium Deposita, v. 25, p. 65–72.

Davis, D.W., 2002. U-Pb geochronology of Archean metasedimentary rocks in the Pontiac and Abitibi Subprovinces, Quebec, Constraints on timing, provenance and regional tectonics; Precambrian Research, v. 115, p. 97–117.

Derry, D.R., 1939. The geology of the Canadian Malartic gold mine, N. Quebec; Economic Geology, v. 34, p. 495–523.

De Souza, S., Dubé, B., McNicoll, V., Mercier-Langevin, P., Dupuis, C., Creaser, R., de Chavigny, P., and Gervais, D., 2013. The Canadian Malartic mine, Abitibi, Quebec: Geological characteristics and relative timing of low-grade bulk-tonnage gold mineralization; Ministère des Ressources Naturelles du Québec, Québec-Mines, Abstracts, p. 28.

De Souza, S., Dubé, B., McNicoll, V., Dupuis, C., Mercier-Langevin, P., Creaser, R., and Kjarsgaard, I., in press, Geology, structure and timing of hydrothermal alteration at the Canadian Malartic Archean stockwork disseminated world-class gold deposit, Quebec, Canada, *In:* Archean Base and Precious Metal Deposits, Southern Abitibi Greenstone Belt, Canada, (ed.) T. Monecke, P. Mercier-Langevin, and B. Dubé; Society of Economic Geologists, Field guide book 46.

Desrochers, J.P. and Hubert, C., 1996. Structural evolution and early accretion of the Archean Malartic composite block, southern Abitibi greenstone belt, Quebec, Canada; Canadian Journal of Earth Sciences, v. 33, p. 1556–1569.

Dubé, B. and Gosselin, P., 2007. Greenstone-hosted quartz-carbonate vein deposits, *In:* Mineral Deposits of Canada: A Synthesis of Major Deposit Types, District Metallogeny, the Evolution of Geological Provinces and Exploration Methods, (ed.) W.D. Goodfellow; Geological Association of Canada, Mineral Deposits Division, Special Publication No. 5, p. 49–73.

Fallara, F., Ross, P.-S., and Sansfaçon, R., 2000. Caractérisation géochimique, pétrographique et structurale: Nouveau modèle métallogénique du camp minier de Malartic; Ministère des Ressources Naturelles du Québec, MB 2000-15, 41 p.

Fallara, F., Ross, P.-S., Sansfaçon, R., and Grant, M., 2005. Lac Fournière; Ministère des Ressources Naturelles du Québec, Geological compilation map, 32D01-200-0102, scale 1: 20,000.

Goldfarb, R.J., Baker, T., Dubé, B., Groves, D.I., Hart, C.J.R., Robert, F., and Gosselin, P., 2005. World distribution, productivity, character, and genesis of gold deposits in metamorphic terranes, *In:* One Hundredth Anniversary Volume, (ed.) J.W. Hedenquist, J.F.H. Thompson, R.J. Goldfarb, and J.P. Richards; Society of Economic Geologists, p. 407–450.

Grant, J.A., 1986. The isocon diagram – a simple solution to Gresens' equation for metasomatic alteration; Economic Geology, v. 81, p. 1976–1982.

Grant, M., Fallara, F., Ross, P.-S., and Sansfaçon, R., 2005. Malartic; Ministère des Ressources Naturelles du Québec, Geological compilation map, 32D01-200-0202, scale 1: 20,000.

Hart, C.J.R., 2007. Reduced intrusion-related gold systems, *In:* Mineral Deposits of Canada: A Synthesis of Major Deposit Types, District Metallogeny, the Evolution of Geological Provinces and Exploration Methods, (ed.) W.D. Goodfellow; Geological Association of Canada, Mineral Deposits Division, Special Publication No. 5, p. 95–112.

Helt, K.M., Williams-Jones, A.E., Clark, J.R., Wing, B., and Wares, R.P., 2014. Constraints on the genesis of the Archean oxidized, intrusion-related Canadian Malartic gold deposit, Quebec, Canada; Economic Geology, v. 109, p. 713–735.

Hodgson, C.J., 1993. Mesothermal lode-gold deposits, *In:* Mineral Deposit Modeling, (ed.) R.V. Kirkham; Geological Association of Canada, Special Paper 40, p. 635–678.

Ispolatov, V., Lafrance, B., Dubé, B., Creaser, R., and Hamilton, M., 2008. Geological and structural setting of gold mineralization in the Kirkland Lake-Larder Lake gold belt, Ontario; Economic Geology, v. 103, p. 1309–1340.

Issigonis, M.J., 1980. Occurrence of Disseminated Gold Deposits in Porphyries in Archean Abitibi Belt, NW Quebec, Canada; Institution of Mining and Metallurgy London, Transactions, Section B: Applied Earth Sciences, v. 89, p. 157–158.

Pilote, P., 2013. Géologie – Malartic; Ministère des Ressources naturelles du Québec, CG-32D01D-2013-01.

Pilote, P., Daigneault, R., David, J., and McNicoll, V., 2014. L'architecture des groupes de Malartic, de Piché et de Cadillac et de la Faille de Cadillac, Abitibi : révision géologique, nouvelles datations et interprétations; Ministère des ressources naturelles du Québec, Québec-Mines, Résumés, DV2014-07.

Poulsen, K.H., Card, K.D., and Franklin, J.M., 1992. Archean tectonic and metallogenic evolution of the Superior Province of the Canadian Shield; Precambrian Research, v. 58, p. 25–54.

Poulsen, K.H., Robert, F., and Dubé, B., 2000. Geological classification of Canadian gold deposits; Geological Survey of Canada, Bulletin 540, 106 p.

Robert, F., 2001. Syenite-associated disseminated gold deposits in the Abitibi greenstone belt, Canada; Mineralium Deposita, v. 36, p. 503–516.

Robert, F., Brommecker, R., Bourne, B.T., Dobak, P.J., McEwans, C.J., Rowe, R.R., and Zhou, X., 2007. Models and exploration methods for major gold deposit types, *In:* Proceedings of Exploration 07: Fifth Decennial International Conference on Mineral Exploration, (ed) Milkereit, B., p. 691-711.

Robert, F., Poulsen, K.H., Cassidy, D.F., and Hodgson, C.J., 2005. Gold metallogeny of the Superior and Yilgarn cratons, *In:* One Hundredth Anniversary Volume, (ed.) J.W. Hedenquist, J.F.H. Thompson, R.J. Goldfarb, and J.P. Richards; Society of Economic Geologists, p. 1001–1033.

Sansfaçon, R. and Hubert, C., 1990. The Malartic gold district, Abitibi greenstone belt, Quebec: Geological setting, structure and timing of gold emplacement at Malartic Gold Fields, Barnat, East Malartic, Canadian Malartic and Sladen Mines *In:* The Northwestern Quebec Polymetallic Belt, (ed.) A. Simard; Canadian Institute of Mining and Metallurgy, Special Volume 43, p. 221–235.

Sansfaçon, R., Grant, M., and Trudel, P., 1987. Géologie de la Mine Canadian Malartic – District de Val d'Or; Ministère des Ressources naturelles du Québec, MB 87-26, 44 p.

Sinclair, W.D., 1982. Gold deposits of the Matachewan Area, Ontario, *In:* Geology of Canadian Gold Deposits, (ed.) R.W. Hodder and W. Petruk; Canadian Institute of Mining and Metallurgy, Special Volume 24, p. 83–93.

Trudel, P., and Sauvé, P., 1992. Synthèse des caractéristiques géologiques des gisements d'Or du district de Malartic; Ministère des Ressources naturelles du Québec, MM89-04, 113 p.

Zhang, J., Lin, S., Linnen, R., and Martin, R., 2014. Structural setting of the Young-Davidson syenite-hosted gold deposit in the western Cadillac-Larder Lake deformation zone, Abitibi greenstone belt, Superior Province, Ontario; Precambrian Research, v. 248, p. 39–59.